



HAL
open science

PAHs increase the production of extracellular vesicles both in vitro in endothelial cells and in vivo in urines from rats

Manon Le Goff, Dominique Lagadic-Gossmann, Remi Latour, Normand Podechard, Nathalie Grova, Fabienne Gauffre, Soizic Chevance, Agnès Burel, Brice M.R. Appenzeller, Lionel Ulmann, et al.

► To cite this version:

Manon Le Goff, Dominique Lagadic-Gossmann, Remi Latour, Normand Podechard, Nathalie Grova, et al.. PAHs increase the production of extracellular vesicles both in vitro in endothelial cells and in vivo in urines from rats. *Environmental Pollution*, 2019, 255, pp.113171. 10.1016/j.envpol.2019.113171 . hal-02302334

HAL Id: hal-02302334

<https://univ-lemans.hal.science/hal-02302334>

Submitted on 20 Jul 2022

HAL is a multi-disciplinary open access archive for the deposit and dissemination of scientific research documents, whether they are published or not. The documents may come from teaching and research institutions in France or abroad, or from public or private research centers.

L'archive ouverte pluridisciplinaire **HAL**, est destinée au dépôt et à la diffusion de documents scientifiques de niveau recherche, publiés ou non, émanant des établissements d'enseignement et de recherche français ou étrangers, des laboratoires publics ou privés.



Distributed under a Creative Commons Attribution - NonCommercial 4.0 International License

40 **Abstract (300 words)**

41 Environmental contaminants, to which humans are widely exposed, cause or worsen several
42 diseases, like cardiovascular diseases and cancers. Among these molecules, polycyclic aromatic
43 hydrocarbons (PAHs) stand out since they are ubiquitous pollutants found in ambient air and diet.
44 Because of their toxic effects, public Health agencies promote development of research studies
45 aiming at increasing the knowledge about PAHs and the discovery of biomarkers of exposure and/or
46 effects.

47 Extracellular vesicles (EVs), including small extracellular vesicles (S-EVs or exosomes) and large
48 extracellular vesicles (L-EVs or microvesicles), are delivery systems for multimolecular messages
49 related to the nature and status of the originating cells. Because they are produced by all cells and
50 detected within body fluids, EV releases could act as cell responses and thereby serve as biomarkers.
51 To test whether EVs can serve as biomarkers of PAHs exposure, we evaluate the effects of these
52 pollutants on EV production using an *in vitro* approach (human endothelial cell line, HMEC-1) and
53 an *in vivo* approach (urine samples from PAHs-exposed rats). Our study indicates that, i) PAH
54 exposure increases *in vitro* the EV production by endothelial cells and *in vivo* the release of EVs in
55 urine, and that the stimulating effects of PAHs concern both S-EVs and L-EVs; ii) PAH exposure and
56 more particularly exposure to B[a]P, can influence the composition of exosomes produced by
57 endothelial cells; iii) the aryl hydrocarbon receptor, a cytosolic receptor associated to most
58 deleterious effects of PAHs, would be involved in the PAH effects on the release of S-EVs, but not L-
59 EVs.

60 These results suggest that EVs may have utility for monitoring exposure to PAHs, and more
61 particularly to B[a]P, considered as reference PAH, and to detect the related early cellular response
62 prior to end-organ damages.

63

64 **Capsule :**

65 Exposure to polycyclic aromatic hydrocarbons, like benzo[a]pyrene, increases, *in-vitro* and *in-vivo*,
66 production of exosomes and microvesicles and modifies their compositions

67 **Keywords :**

68 Polycyclic aromatic hydrocarbons, Aryl hydrocarbon receptor, Endothelial cells, Urine, Extracellular
69 vesicles, Exosomes, Microvesicles, Large EVs, Small EVs

70

71 **Highlights**

- 72
- 73 • B[a]P stimulates EV production by endothelial HMEC-1 cells.
 - 74 • B[a]P stimulates production of both S-EVs (exosomes) and L-EVs (microvesicles).
 - 75 • B[a]P modifies protein cargoes of S-EVs.
 - 76 • S-EV, but not L-EV, increased production by B[a]P is AhR dependent.
 - 77 • *In vivo* exposure to PAHs increases urinary EV amount.

77

78

79 1. Introduction

80 Nowadays, there is broad consensus regarding the fact that our environmental health markedly
81 depends on the impact of environmental contaminants to which humans are widely exposed¹,
82 especially *via* diet and ambient air. Most of these chemicals, such as heavy metals, persistent organic
83 pollutants and biocides, come from anthropogenic activities. They are known to cause or worsen
84 several diseases, like cardiovascular diseases (CVD), immune dysfunctions and cancers². Among
85 these molecules, polycyclic aromatic hydrocarbons (PAHs) stand out since they are ubiquitous
86 pollutants notably found in ambient air and diet. They are involved in the occurrence of human
87 CVDs, and exhibit immunotoxic, mutagenic, and carcinogenic properties³. Most deleterious effects
88 of PAHs are related to their binding to the aryl hydrocarbon receptor (AhR), a cytosolic ligand-
89 activated transcription factor. PAH binding to this receptor triggers a canonical genomic pathway
90 with the nuclear translocation of AhR followed by its interaction with aryl hydrocarbon receptor
91 nuclear translocator (ARNT), thus allowing its binding to specific genomic elements termed
92 xenobiotic responsive elements (XREs). XREs are found in the promoter of PAHs-responsive genes,
93 such as cytochromes P-450 (CYP) 1A1 and 1B1, that are known carcinogen bioactivating enzymes.
94 AhR activation also triggers several non-genomic pathways, including intracellular calcium signaling
95 and tyrosine kinase SRC activation^{4,5}. The United States Environmental Protection Agency (US-EPA)
96 as well as the World Health Organization (WHO) consider some of PAHs as priority pollutants due
97 to their critical effects on human health⁶. This has led to the development of research studies aiming
98 at increasing the knowledge about these molecules and the discovery of biomarkers of exposure
99 and/or effects.

100 During the last decade, extracellular vesicles (EVs) have drawn an increasing attention in the
101 field of biomarkers of diseases or exposure to xenobiotics⁷⁻¹¹. Theoretically produced by all cells,
102 EVs, including small extracellular vesicles (S-EVs or exosomes) and large extracellular vesicles (L-EVs
103 or microvesicles), are delivery systems for multimolecular messages closely related to the nature

104 and status of originating cells^{12,13}. These cellular nanostructures are differentiated by their size (S-
105 EV: less than 200 nm, L-EV: less than 1000 nm), their biogenesis processes (S-EV: generated within
106 endosomal compartments , L-EV: budding from the plasma membrane) and by their components
107 (lipids, proteins, DNAs, mRNAs, miRNAs...)¹⁴. EVs allow intercellular communication and
108 consequently are involved in many biological processes such as cell maintenance and proliferation,
109 tissue repair, angiogenesis... They have been detected within body fluids (i.e. blood, urine, lymph,
110 saliva...) in healthy humans but also in patients^{15,16}. In this latter case, EV production is exacerbated
111 and their content altered. Such alterations notably occur during cancer, metabolic,
112 neurodegenerative or CVDs^{17,18} .

113 The EV overproduction is also observed during exposure to xenobiotics. Thus, some drugs or
114 toxicants (like acetaminophen, alcohol, diclofenac or cigarette smoke) are able to increase *in vitro*
115 and/or *in vivo* EV production, and to change their composition¹⁹⁻²². As a consequence, EVs could
116 serve as biological markers of cell responses and possibly even susceptibility to toxicity. They also
117 offer the possibility of detecting toxicity at the very early stages of development before irreversible
118 effects occur.

119 Although the molecular mechanisms still remain to be fully clarified, there is evidence
120 showing that an increase in intracellular calcium concentration ($[Ca^{2+}]_i$), plasma membrane
121 remodeling or oxidative stress are involved in the EV release by cells^{23,24}. Interestingly, we previously
122 reported that PAHs and more specifically the prototypical PAH, benzo[a]pyrene (B[a]P), can trigger
123 such cellular events. Indeed, our team previously demonstrated that cell exposure to various PAHs
124 can increase the $[Ca^{2+}]_i$, *via* an AhR-independent activation of the β 2-adrenergic receptor²⁵, and that
125 membrane remodeling (characterized by an increase in fluidity and destabilization of lipid rafts), is
126 a key mechanism in the B[a]P-associated toxicity²⁶.

127 Exposures to xenobiotics or lifestyle factors, such as air pollutants²⁷ cigarette smoke²⁸,
128 alcohol¹⁹, or high fat diet²⁹, would be able to modify EV trafficking, the amount produced and

129 composition (e.g. proteins, miRNA), notably in biological fluids such as plasma or urine. In this
130 context, circulating EVs might provide information about both exposure level and toxic responses
131 of the organism. EVs in blood plasma of healthy humans mainly originate from platelets.
132 Comparatively, endothelial cells produce few EVs³⁰. However, while the level of EV production by
133 these latter cells is low under physiological conditions, it can considerably increase in pathological
134 situation³⁰. Thus, the amount of endothelium-derived EVs circulating in the blood stream has been
135 shown to correlate with the severity of diverse diseases, eg. sepsis, stroke, atherosclerosis and
136 metabolic syndrome ¹⁷. Endothelial cells are also particularly interesting to focus on since they also
137 participate in the production of EVs detected in urine^{31,32}. It is within this framework that our study
138 was carried out.

139 In order to test whether EVs can serve as biomarkers of PAH exposure, the present study was
140 designed to evaluate the effects of these pollutants on EV production. To this aim, two different
141 approaches were applied: i) an *in vitro* approach, using the human endothelial cell line HMEC-1; and
142 ii) an *in vivo* approach, using urine samples obtained from PAH-exposed rats. Urine provides a good
143 alternative to blood in the field of disease biomarkers because this biological fluid can be collected
144 noninvasively and in large amounts³³. Our present data demonstrate that PAHs can increase EV
145 production by endothelial cells. This overproduction observed *in vitro* concerns both S-EVs and L-
146 EVs probably involving different molecular mechanisms. Indeed, it seems that only the increase of
147 S-EVs would be AhR-dependent. Moreover, the PAH-related increase in EV production was also
148 observed *in vivo* in urine samples from rats exposed to the 16 PAHs listed as “priority” compounds
149 by US-EPA.

150 **2. Materials and Methods**

151 **2.1. Chemicals and Reagents**

152 Benzo[e]pyrene (B[e]P), pyrene (PYR), benz[a]anthracene (B[a]A), benzo[a]pyrene (B[a]P),
153 dibenz[*a,h*]anthracene (DBA), chrysene, benzo[b]fluoranthene, benzo[k]fluoranthene,
154 benzo[*g,h,i*]perylene, indeno[1,2,3-*c,d*]pyrene, naphthalene, fluorene, acenaphthene,
155 acenaphthylene, anthracene, phenanthrene, fluoranthene, alpha-naphthoflavone (α -NF), dimethyl
156 sulfoxide (DMSO) and monoclonal antibody anti- β -actin were obtained from Sigma-Aldrich (St.
157 Louis, MO, USA). Antibodies against CD63, lamin A/C and Hsc70 were from Santa Cruz Biotechnology
158 (Santa Cruz, CA, USA), whereas Tsg101 was provided by Abcam and caveolin-1 and flotillin-1 by BD
159 biosciences. All other chemicals used in this study were purchased from commercial sources at the
160 highest purity available.

161 **2.2. Cell Culture**

162 The Human Microvascular Endothelial Cell line (HMEC-1) was obtained from the Center for Disease
163 Control and Prevention (Atlanta, GA). Cells were routinely maintained in MCDB-131 medium
164 containing hydrocortisone (1 μ g/mL), epidermal growth factor (10 ng/mL), penicillin (50 unit/mL),
165 streptomycin (50 unit/mL), L-glutamine (10 mM), and supplemented with 10% fetal bovine serum
166 (FBS). At 90% confluence, before each treatment, cells were cultured overnight in serum-free
167 medium. Chemicals were prepared as stock solutions in DMSO. The final concentration of vehicle
168 did not exceed 0.2% (v/v); control cultures received the same concentration of DMSO. In all
169 experiments using chemical inhibitors, cells were pre-treated 1 hour prior to and during exposure.

170 **2.3. Animal experimentation**

171 Long Evans rats (female of 180-200 g, Elevage Janvier, St Berthevin, France) were housed in plastic
172 cages under controlled environment (12 h light/dark cycle, light on at 7 am, temperature of $22 \pm 2^\circ\text{C}$

173 and relative humidity of 40 ± 5 %). Food and water were available *ad libitum*. The water, food and
174 oil were tested according to NF ISO 15302 to confirm that all these matrices were PAH-free down
175 to a detection limit of 10 ng/L of water and 1 ng/g of fat. Rats were acclimatized to the animal facility
176 for 2 weeks prior to experiment onset. The mix of PAHs was composed of the 16 compounds pointed
177 out the US-EPA for their toxicity, and prepared in vegetable oil weekly (ISIO4, Lesieur, Neuilly-sur-
178 Seine, France). Treatment of animals has been described in a previous study³⁴. Briefly, four rats were
179 randomly allocated to each of the experimental group receiving 0.8 mg/kg body weight of each
180 compound included in the mix, by oral administration, 3 times per week over a 90-day period.
181 Control rats received only vehicle. At the end of 90 days-experiment, urine fractions were collected
182 after 24 h in refrigerated tubes and storage at -20°C . All procedures were conducted in accordance
183 with European Communities Council Directive of 22 September 2010 (2010/63/EU) and approved
184 by the Ministry of Agriculture, Grand-Duchy of Luxembourg.

185 **2.4. Isolation of EVs from HMEC-1 cells**

186 Cells were cultured using cell culture petri dishes of 151.9 cm^2 (CorningTM, Thermo Fisher Scientific,
187 France). After PAH exposure, in order to isolate total EVs, L-EV or S-EV, the serum-free conditioned
188 medium was first centrifuged at $3650 \times g$ for 10 min to remove cells and cell debris and obtain the
189 cell-cleared supernatants. Total EVs were pelleted by direct ultracentrifugation of the culture media
190 at $100,000 \times g$ for 1h45 at 4°C (Beckman Coulter Optima L-90K Series Ultracentrifuges, rotor Sw
191 28.1); the pellet was then resuspended in sterile phosphate-buffered saline (PBS), followed by
192 another centrifugation at $100,000 \times g$ for 1h45 min at 4°C . Total EV pellets were finally resuspended
193 in sterile PBS.

194 L-EVs were recovered from cell-cleared supernatants following centrifugation at $10\ 000 \times g$ for 30
195 min, followed by one washing step in PBS at $10\ 000 \times g$ for 30 min, and then resuspended in sterile
196 PBS. S-EVs were further isolated from L-EVs-depleted supernatants following filtration at $0.2\ \mu\text{m}$

197 and a 100 000 x g ultracentrifugation step for 1h45 at 4°C, followed by one washing step in PBS at
198 100 000 x g for 1h45, and then resuspended in sterile PBS.

199 **2.5. Isolation of urine EVs**

200 About 9 mL of urine were first diluted half in PBS and centrifuged at 300 x g for 10 min, then 2 000
201 x g for 10 min to remove cells and cell debris. EVs were pelleted by ultracentrifugation at 100 000 x
202 g for 2 h at 4°C (Beckman Coulter Optima L-90K Series Ultracentrifuges, rotor Sw 28.1). The pellet
203 was next resuspended in sterile PBS containing dithiothreitol (DTT; 200 mg/mL) at 37°C for 10
204 minutes in order to dissociate of uromodulin aggregates^{35,36}, and then resuspended in sterile PBS,
205 followed by another centrifugation at 100 000 x g for 2h at 4°C. Total EV pellets were finally
206 resuspended in sterile PBS.

207 **2.6. Nanoparticle tracking analysis**

208 EV samples were diluted in sterile PBS before nanoparticle tracking analysis (NTA). Size distribution
209 and vesicle concentration were determined by NTA using a NanoSight LM14 (Malvern Instruments,
210 Malvern, UK). A 405 nm laser beam is used to highlight the samples. Three 30 s captures per sample
211 were recorded at 25°C. Videos were analysed using NanoSight NTA 3.1 software (Malvern, UK) using
212 a detection threshold set to 3. The presented results correspond at least to an average from three
213 videos for each of three independent samples of EVs, S-EVs and L-EVs. EV concentrations and
214 distributions were then normalized to the cell count and expressed as number of EVs released per
215 cell.

216 **2.7. Electron microscopy**

217 Transmission electron microscopy (TEM) was performed as described by Théry et al.³⁷. Briefly, S-EVs
218 and L-EVs were resuspended in 2% paraformaldehyde (PFA). Formvar-carbon coated copper grids
219 (Agar Scientific, Stansted, UK) were placed on 5 µL S-EVs or L-EVs suspension for 20 min and washed

220 with PBS. Vesicles were fixed in 1% glutaraldehyde in PBS for 5 minutes. After washing with distilled
221 water, grids were placed on a drop of uranyl-oxalate for 5 min and of ice-cold 2% methyl cellulose/
222 4% uranyl acetate (1/9; v/v) for 10 min. EVs were visualized using a JEOL JEM-1400 transmission
223 electron microscope (JEOL, Japan).

224 **2.8. Annexin V binding analysis**

225 Staining by Annexin V-phycoerythrin (annexin V-PE, BD Pharmingen™) has been used to detect
226 phosphatidylserine at the L-EV surfaces. An analysis window was defined using beads (Megamix,
227 Stago) of diameters 0.5 µm, 0.9 µm and 3 µm. To determine the Annexin V positivity, L-EVs were
228 incubated with Annexin V-PE, counting beads (Flow-Count™ Fluorospheres, Beckman) and buffer
229 (14 mM NaCl, 10 mM HEPES, 2.5 mM calcium). Labelling in the absence of calcium was used as
230 negative control. L-EVs stained with annexin V-PE were then analyzed by a BD FACSCanto™ III
231 cytometer. Data have been exported using BD FACSDiva™ software.

232 **2.9. Western Blotting**

233 Total cellular, S-EV and L-EV protein amounts were estimated by a BCA Protein Assay Kit (Thermo
234 Fisher Scientific, UK), using BSA as a standard. 5 µg proteins were separated by sodium dodecyl
235 sulfate–polymerase gel electrophoresis (SDS–PAGE), and electrophoretically transferred onto
236 nitrocellulose membranes (Merck Millipore). After blocking with a Tris-buffered saline solution
237 supplemented with 2% bovine serum albumin for 2 h, membranes were hybridized with primary
238 antibodies overnight at 4°C. Membranes were then incubated with horseradish peroxidase-
239 conjugated secondary antibodies for 1 h. Immunolabeled proteins were visualized by
240 chemiluminescence using the LAS-3000 analyzer (Fujifilm) or Molecular Imager ChemiDoc™ XRS+
241 (Bio-Rad). Image processing was performed using Multi Gauge software (Fujifilm) or Image Lab™
242 software (Bio-Rad). For protein loading evaluation, a primary antibody against HSC70 was used.

243 **2.10. Intracellular Calcium Concentration Measurements**

244 Cells used for intracellular calcium concentration ($[Ca^{2+}]_i$) measurements were grown on glass
245 coverslips. The glass coverslips were sterilized in ethanol of increasing concentrations from 70 to
246 99%, and then coated with serum proteins using pure FBS prior to cell culture. Variations in $[Ca^{2+}]_i$
247 were analyzed in PAH-exposed HMEC-1 cells by real time fluorescence imaging, using Ca^{2+} -sensitive
248 probe Fura-2-AM, as previously reported^{25,38}. Briefly, cells were incubated at 37°C (30 min) in cell
249 suspension buffer supplemented with 1.5 μ M Fura-2AM and 0.006% pluronic acid. Changes in $[Ca^{2+}]_i$
250 were monitored using a DMIRB (Leica, Wetzlar, Germany) inverted microscope-based imaging
251 system equipped with a 40 \times /1.35 UApo N340 high UV light transmittance oil immersion objective
252 (Olympus, Waltham, MA, USA), a CoolSnapHQ fast-cooled monochromatic digital camera (Princeton
253 instrument), a DG-4 Ultra High Speed Wavelength Switcher (Sutter Instruments, Novato, CA, USA)
254 for fluorophore excitation, and METAFLUOR software (Universal Imaging, Downingtown, PA, USA)
255 for image acquisition and analysis. The $[Ca^{2+}]_i$ imaging involved data acquisition every 10 s (emission
256 at 510 nm) at 340- and 380-nm excitation wavelengths. The ratio of fluorescence intensities
257 recorded after excitation at 340 nm (F340) and 380 nm (F380) was used to estimate intracellular
258 calcium concentrations. $[Ca^{2+}]_i$ data were expressed as normalized maximum delta ratio, i.e., the
259 difference between the basal level of $[Ca^{2+}]_i$ -related fluorescence ratios (F340/F380) before DMSO
260 or PAH treatment and the maximum level of $[Ca^{2+}]_i$ -related fluorescence ratios (F340/F380)
261 obtained during DMSO or PAH treatment.

262 **2.11. Apoptosis**

263 Cells used for apoptosis analysis were cultivated in 6-well plates. Hoechst 33342/Sytox green
264 staining was carried out to observe apoptotic cells by fluorescence microscopy. After PAH exposure,
265 cells were stained with 50 μ g/mL Hoechst 33342 and 93.5 nM Sytox green in the dark at 37°C for 30
266 min. More than 300 cells in randomly selected microscopic fields were analyzed and were scored

267 under ZEISS Axio Scope A1 microscope. Cells with condensed or fragmented chromatin were
268 counted as apoptotic.

269 **2.12. RNA Isolation and Analysis**

270 Total RNA was isolated from cells using the TRIzol® reagent (Invitrogen, Cergy Pontoise, France) and
271 then reverse-transcribed using the High-Capacity cDNA Reverse Transcription Kit (Life Technologies,
272 Carlsbad, CA, USA). Real-time quantitative PCR (RT-PCR) was performed using SYBR Green PCR
273 Master Mix on the CFX384 Touch™ Real-Time PCR Detection System (Bio-Rad, Hercules, CA, USA).
274 The mRNA expressions were normalized by means of 18s mRNA levels. The $2^{-\Delta\Delta Ct}$ method was used
275 to express the relative expression of each selected gene. Primers were as follows: CYP1A1-forwards:
276 5'- CCCACAGCACAACAAGAGACA-3'; CYP1A1-reverse: 5'-CATCAGGGGTGAGAAACCGT-3'; CYP1B1-
277 forwards: 5'-AGCCAGGACACCCTTTCC-3'; CYP1B1-reverse: 5'-GAGTTGGACCAGGTTGTG-3'; 18S-
278 forwards: 5'-CGCCGCTAGAGGTGAAATTC-3'; 18S-reverse: 5'-TTGGCAAATGCTTTTCGCTC-3'.

279 **2.13. Statistical analysis**

280 All values were presented as means \pm SEM from at least 3 independent experiments. Statistical
281 analysis was performed using Student's *t* test and the one-way ANOVA with Dunnett's post hoc test
282 (GraphPad Prism5, GraphPad Software, Inc, San Diego, California, USA). Significance was accepted
283 at $p < 0.05$.

284

285 **3. Results**

286 **3.1. B[a]P stimulates the production of EVs by endothelial HMEC-1 cells.**

287 Endothelial cells constitute a well-known target for PAHs^{25,39}, and are part of the cells mainly
288 producing EVs under physiological conditions³⁰. We therefore decided to explore effects of B[a]P on
289 EV production by the endothelial HMEC-1 cells using different concentrations and times of
290 treatment. NTA revealed that B[a]P significantly stimulated EV production by HMEC-1 cells from 100
291 nM (Fig.1A) and after 12h of treatment (Fig.1B). After 24h of treatment with 100 nM B[a]P,
292 observation by NTA of the size distribution profile of EVs (Fig.1C) showed that they exhibited
293 diameters ranging from 50 nm to 600 nm, and that B[a]P stimulated the production of the entire
294 population of EVs (regardless of EV size).

295 **3.2. B[a]P stimulates the production of both S-EVs and L-EVs by endothelial HMEC-1 cells**

296 It is known that cells can release a heterogeneous population of vesicles with variable diameters
297 and different biogenesis processes, including small EVs (i.e. exosomes) formed inside endosomal
298 compartments and larger EVs (i.e. microvesicles) budding from the plasma membrane. To get more
299 insight into the characterization of the EV overproduction in treated HMEC-1 cells, we next
300 evaluated the B[a]P effect by looking at both small (diameter <200 nm) and large (diameter >200
301 nm) EVs, following differential ultracentrifugation and filtration through 0.22 μ m filters. Thus, our
302 experimental procedure allowed us to isolate two populations of EVs: the small EV population (S-
303 EVs) corresponding to EVs with average diameter of 160.1 ± 12.6 nm, and the large EV population
304 (L-EVs) corresponding to EVs with average diameter of 295.8 ± 13.2 nm. Whereas B[a]P exposure
305 (100 nM, 24h) did not change EV diameters (Fig. S1), it nonetheless increased the production of
306 both S-EVs and L-EVs (Fig. 2A and 2B respectively), to the same extent (by about 2 fold) as for total
307 EVs (Fig.1B).

308 **3.3. S-EV and L-EV populations isolated from HMEC-1 cells correspond respectively to** 309 **exosomes and microvesicles**

310 In order to test whether S-EVs and L-EVs isolated under our experimental conditions correspond
311 respectively to exosomes or microvesicles, we next examined their morphology and composition.
312 As expected, TEM images revealed structures with expected cup-shaped appearance and diameters
313 (Fig. 3A). By western blotting (Fig. 3B), using total cell lysates as positive controls, we failed to detect
314 any lamin A/C in isolated S-EVs and L-EVs, thus ruling out a possible contamination of our EV samples
315 by nucleus material. In contrast, proteins traditionally observed in both exosomes and microvesicles
316 such as caveolin-1, flotillin-1, β -actin, Tsg101 and HSC70 (used as loading control), were detected in
317 both S-EVs and L-EVs. Finally, a protein described to be more specific to exosome, that is CD63, was
318 only detected in S-EVs (Fig. 3B) and cell lysates. It is known that microvesicles expose
319 phosphatidylserine on their outer leaflet of the membrane^{40,41}; therefore we next used the
320 fluorescently labeled annexin V to analyze its presence in L-EVs (Fig. 3C). By flow cytometry, we
321 found that 69 ± 3.6 % of isolated L-EVs were annexin-V positive.
322 Altogether, these observations indicated that our technical procedure allowed the isolation of S-EVs
323 and L-EVs corresponding respectively to exosome- and microvesicle-enriched populations produced
324 by HMEC-1 cells.

325 **3.4. B[a]P would modify the protein cargoes of EVs produced by HMEC-1**

326 In parallel to the characterization of S-EVs et L-EVs produced by HMEC-1 cells, we also investigated
327 whether the EV composition and characteristics studied were affected by B[a]P exposure. At first,
328 we found that no significant modification was observed in presence of B[a]P when looking at EV
329 morphologies (Fig. 3A) or annexin V labeling (Fig. 3C). To analyze the protein cargoes of EVs, 5 μ g of
330 total proteins were subjected to SDS-PAGE western blotting to compare protein composition of S-
331 EV or L-EVs produced by cells in presence or not of B[a]P (Fig. 3B). Cell lysates were used as positive
332 control. Among the studied proteins, the levels of caveolin-1, flotillin-1 or β -actin appeared to be
333 increased in EVs produced upon B[a]P exposure, especially in S-EVs. The densitometric analysis thus

334 revealed that caveolin-1 and flotillin-1 inductions were significant in the presence of this PAH
335 (Fig.S2).

336 **3.5. The increased production of S-EVs, but not L-EVs, upon B[a]P exposure would be AhR-**
337 **dependent and calcium-independent**

338 PAHs are known to trigger numerous interconnected cellular phenomena, associated or not to AhR
339 activation, among them the induction of xenobiotic-metabolism enzymes, intracellular calcium
340 signaling, membrane remodeling or apoptotic signaling^{5,42,43}. Interestingly, several of them are also
341 implicated in the production of EVs by cells. Thus, upon cell activation or apoptosis, the increase of
342 $[Ca^{2+}]_i$ underlies the initiation of cell signaling pathways, remodeling of cytoskeleton and the
343 redistribution of membrane phospholipids associated to the intracellular processing for exosome
344 and/or microvesicles release⁴⁴. To get further insight into the possible mechanisms involved in the
345 EV production upon B[a]P exposure, we decided to focus our attention on AhR activation, calcium
346 signal and apoptosis.

347 ***Only AhR ligands can increase EV production by HMEC-1 cells.*** In order to test the possible
348 involvement of AhR, we first decided to evaluate the potential of several PAHs with different AhR
349 affinities, to increase EV production in HMEC-1 cells. To this aim, benzo[e]pyrene (B[e]P), pyrene
350 (PYR), benz[a]anthracene (B[a]A) and dibenzo[a,h]anthracene (DBA) were chosen because they are
351 part of the 16 U.S EPA priority pollutant PAH compounds; they are present in diet and possess
352 different levels of affinity for AhR, therefore resulting in different potencies in terms of genomic
353 AhR activation as compared to B[a]P (Fig. S3). The amount and size distribution of EVs produced by
354 HMEC-1 cells were thus studied after 24 h of treatment with 100 nM of each PAH. Before focusing
355 on EVs, we first evaluated the potential for AhR activation of our PAHs by studying the induction of
356 known AhR-target genes, i.e. CYP1A1 and 1B1 (Fig. 4A). As expected, only B[a]A, B[a]P, and DBA
357 (AhR ligands) induced CYP1A1 and 1B1 mRNA levels. The other PAHs tested (B[e]P and PYR), known
358 to exhibit a very low affinity for AhR, failed to modify the expression of CYP1A1 and 1B1 in our cell

359 model. Interestingly, like B[a]P, B[a]A and DBA were both capable of increasing the EV production
360 by HMEC-1 cells in contrast to B[e]P and PYR which were ineffective (Fig. 4B). Note that, whatever
361 the PAH tested, analysis of the size distribution profile of EVs (Fig. 4C-F) indicated that isolated EVs
362 had diameters ranging from 50 to 600 nm and that, when PAHs exhibited an effect on EV production,
363 this concerned the entire population of EVs (whatever the size of EVs) (Fig.4E, 4F). To determine if
364 a higher concentration of PAHs with low affinity for AhR was able to stimulate EV production by
365 HMEC-1 cells, we decided to expose cells to 1 μ M of PYR for 24h. Even at this high concentration,
366 PYR failed to modify the EV production by HMEC-1 cells (Fig. S4A). This result thus confirms our data
367 with 100 nM, and is concordant with recent publication from our group⁴⁵. Indeed, we have recently
368 demonstrated that PYR was able to increase S-EV production by hepatocytes independently of AhR,
369 and through a Constitutive Androstane Receptor (CAR)-dependent mechanism. Interestingly, unlike
370 hepatocytes, mRNAs of CAR were not detected in HMEC-1 cells (Fig. S4B).

371 ***An AhR antagonist (alpha-naphthoflavone) inhibits the production of S-EVs but not that of L-EVs***
372 ***induced by B[a]P.*** It is noteworthy that the PAH capacity to increase the mRNA levels of CYP1A1 and
373 1B1 dovetail with their capacity to increase the EV production by HMEC-1 cells. These observations
374 led us to hypothesize an implication of AhR in the increased EV production upon B[a]P exposure. To
375 test this hypothesis, we next investigated the effects of α -NF (antagonist of AhR and inhibitor of
376 CYP1) on the B[a]P-triggered induction of S-EVs or L-EVs. As shown in Fig. 5, α -NF (10 μ M)
377 counteracted the up-regulation of S-EVs observed in presence of B[a]P (Fig.5A), while it failed to
378 reduce the L-EV production (Fig. 5B). Interestingly, treatment by 6-formylindolo[3,2-b]carbazole
379 (FICZ, 100 nM, 24h), a potent high affinity ligand of AhR, further supported this finding. Indeed, FICZ
380 was able to increase the production of S-EVs but not that of L-EVs (Fig. S5). Therefore, AhR activation
381 would be involved in the B[a]P-induced production of S-EVs but not of L-EVs, thus suggesting
382 differential mechanisms.

383 ***PAH capacities to induce intracellular calcium concentration do not overlap their capacities to***
384 ***induce EV production.*** Knowing that calcium can be involved in EV production^{18,44} and that B[a]P
385 can increase $[Ca^{2+}]_i$ in HMEC-1 cells²⁵, we next decided to monitor the early $[Ca^{2+}]_i$ changes in
386 response to our test PAHs. To do so, we used a real-time-fluorescence imaging method and the
387 calcium-sensitive probe Fura2-AM. As previously described²⁵, B[a]P (100 nM) was able to increase
388 $[Ca^{2+}]_i$ in HMEC-1 cells (Fig. 6A). The maximum of increase occurred after about 20 min of exposure
389 to B[a]P (Fig. S6). We then analyzed the effects of 100 nM of all other tested PAHs, on $[Ca^{2+}]_i$ in order
390 to determine the maximum level of $[Ca^{2+}]_i$ increase upon exposure to each molecule. Except for
391 DBA, despite differences in terms of kinetics (Fig. S6), all PAHs were able to increase $[Ca^{2+}]_i$ in HMEC-
392 1 cells, to the same extent as B[a]P (Fig. 6A). It is noteworthy that there was no correlation between
393 PAH capacities to elevate $[Ca^{2+}]_i$ and those to increase EV production (Fig. 4B). Thus, B[e]P and PYR
394 were found to induce $[Ca^{2+}]_i$ but failed to modify EV production by HMEC-1 cells; DBA stimulates EV
395 production but did not modify $[Ca^{2+}]_i$; and B[a]P or B[a]A induced both $[Ca^{2+}]_i$ and EV production.
396 Therefore, the early calcium signal triggered by PAHs would likely not be involved in the increased
397 EV production, whatever the type of EVs considered.

398 ***PAH capacities to induce apoptosis do not overlap their capacities to induce EV production.*** As
399 induction of CYP1A1 et 1B1 following AhR activation by PAHs could lead to apoptotic signaling⁴⁶, we
400 then decided to evaluate apoptosis following PAH exposures (100 nM, 24 h). This was performed
401 using fluorescence microscopy and Hoechst/Sytox green staining (Fig.6B). Consistent with literature,
402 100 nM B[a]P slightly (around 5%) but significantly increased the percentage of apoptotic cells. In
403 contrast, the other tested PAHs, i.e. B[e]P, PYR, B[a]A and DBA, did not affect the apoptosis level.
404 As for $[Ca^{2+}]_i$ induction, we therefore noted that there was no correlation between PAH capacities
405 to induce apoptosis and PAH capacities to increase EV production by HMEC-1 cells.

406 **3.6. *In vivo* exposure to a mixture of PAHs increases urinary EV amount**

407 EVs are widely found in all body fluids including blood, saliva or urine⁴⁴. Urine appears as non-
408 invasive source for information reflecting the physio-pathological state of urinary system but also
409 of other physiological systems. Based upon the fact that endothelial cells are part of kidney intrinsic
410 cells producing urinary EVs (uEVs) and that humans are widely exposed to PAH mixture, we finally
411 decided to test the *in vivo* effect of a mixture of the 16 PAHs listed as “priority” compounds by US-
412 EPA, on the amount of EVs in rat urine samples. Thus, we evaluated uEVs amounts in urines collected
413 during 24 h from rats exposed through diet for 90 days to 0.8 mg/kg of PAH mixture in comparison
414 to control rats receiving only vehicle (vegetal oil). After isolation, uEV amounts were analyzed by
415 NTA. As shown in Fig. 7A, rat exposure to PAH mixture led to an increase of uEVs number
416 ($2.39 \cdot 10^9/\text{mL}$ vs $1.30 \cdot 10^9/\text{mL}$) without any significant modification of renal functions, as determined
417 by measuring urinary creatinine concentration and urinary volume (Fig. 7B and C).

418 4. Discussion

419 The growing interest for EVs originates (1)-from works demonstrating that EVs carry a plethora of
420 bioactive molecules (i.e. nucleic acid, lipids, carbohydrates, proteins...) that play roles in cell-to-cell
421 communication, and (2)-from works revealing the clinical interest of EVs as non-invasive diagnostic
422 biomarkers in some human pathologies including cancer⁴⁷. In this context, our study was performed
423 in order to evaluate the capacity of PAHs to increase EV production both *in vitro* and *in vivo* with the
424 aim of determining if these entities could represent potential biomarkers of exposure and/or effects
425 of PAHs.

426 The present study highlights for the first time the capacity of PAHs to increase *in vitro* the EV
427 production by endothelial HMEC-1 cells. Interestingly, only PAH ligands for AhR (i.e. B[a]P, B[a]A,
428 DBA) led to this EV overproduction. Indeed, B[e]P and PYR, that are known weak AhR ligands, failed
429 to modify such a production. Besides AhR activation, several PAHs can induce an intracellular
430 calcium signaling²⁵ and trigger apoptosis²⁶, two cellular phenomena previously related to EV
431 biogenesis^{23,24}. Regarding influence of B[e]P, PYR, B[a]P, B[a]A, or DBA on intracellular calcium
432 concentration, cell apoptosis and CYP1A1/1B1 mRNA levels, our results do support an AhR
433 implication. Indeed, in contrast to the capacities to trigger an early [Ca²⁺]_i increase (as observed in
434 presence of B[e]P, PYR, B[a]P, B[a]A) and apoptosis (as observed only in presence of B[a]P), the PAH
435 capacity to induce mRNA levels of CYP1A1 and 1B1 overlaps that to increase the EV production. These
436 metabolism enzymes are well recognized as being under AhR control⁵ and key actors in B[a]P
437 induced apoptosis²⁶, and, like EVs, are induced in our cell model only by strong AhR ligands.
438 Interestingly, only the increase of S-EV production was significantly counteracted by α -NF (AhR
439 antagonist and inhibitor of CYP1), thus indicating that only the S-EV overproduction by B[a]P-treated
440 HMEC-1 cells would be AhR dependent. These results therefore strengthen the fact that S-EV and L-
441 EV biogenesis processes would differ, as previously proposed by other groups⁴⁸It remains to
442 determine the precise role for AhR in the S-EV production by HMEC-1 cells, notably in presence of

443 B[a]P. Many hypotheses could be considered. Thus, a possible involvement of the sphingolipid
444 pathway would be particularly interesting to evaluate since, in epithelial cells, several AhR ligands,
445 including PAHs, are able to promote the generation of sphingosine-1-phosphate, a bioactive
446 intermediate of sphingolipid metabolism^{49,50}. Indeed, sphingolipids and the enzymes related to their
447 biosynthesis have been associated to EV biogenesis and release, especially by shaping membrane
448 curvature⁵¹. Another hypothesis might involve a change in the physicochemical characteristics of
449 lipid raft microdomains. Indeed, these entities, that are detected in EV membranes²³, represent
450 assemblies of proteins and lipids within the plasma membrane that are notably enriched in
451 cholesterol and sphingolipids⁴⁰; most interestingly, they are elements of the regulatory mechanisms
452 associated to the vesicle formation and structure²³. As we have previously demonstrated that B[a]P
453 alters the composition of the plasma membrane lipid microdomains notably through AhR
454 activation²⁶, it could be interesting to test a role for such a membrane remodeling in the production
455 of S-EVs by Hmec-1 cells. Of note, the present results indicate that B[a]P exposure could modify EV
456 protein cargoes, notably leading to an enrichment of caveolin-1 and flotillin-1 contents in S-EVs.
457 Interestingly, caveolin-1 and flotillin-1 are well-known markers of lipid rafts. Although studies of
458 greater extent (i.e. proteomics) are needed to conclude, besides stimulating EV production, it seems
459 that PAHs would moreover be able to modify the messages carried by the vesicles by modifying the
460 composition of EVs.

461 Stimulating effects of PAHs, and more particularly B[a]P, towards EV production, concern the
462 two main populations, namely S-EVs and L-EVs, as demonstrated by our EV characterization. As
463 described in the literature, L-EV population (presently observed whatever the treatment applied),
464 is relatively heterogonous as compared to the S-EV population. Looking only at their amount, L-EVs
465 represent less than 20% of total EVs produced by HMEC-1 cells, whereas S-EVs represent more than
466 50%. Note that B[a]P treatment did not significantly affect this distribution (data not shown). Thus
467 in terms of amount, S-EVs would represent the main type of EVs produced by HMEC-1 cells.

468 Nevertheless, considering averaged diameters (160 nm versus 300 nm for S-EVs and L-EVs
469 respectively) and the corresponding averaged membrane surface area (0.08 μm^2 and 0.28 μm^2 for
470 S-EVs and L-EVs respectively), it seems that L-EVs would not be a marginal population considering
471 all EVs produced by HMEC-1. Since PAHs are environmental contaminants with numerous toxic
472 effects on human cells, it could be interesting to determine if the observed L-EV overproduction is
473 an attempt of exposed cells to remove B[a]P. Indeed, the microvesicle trafficking has been
474 previously proposed as a biological process that helps cells to extrude potentially toxic xenobiotics⁵²,
475 thus affording them a means of protection against an intracellular stress. This phenomenon is
476 notably exploited by cancers cells as a mechanism of resistance. Indeed, microvesicles released from
477 cancer cells, after drug treatment (i.e. doxorubicin), contain high levels of the chemotherapeutic
478 agent⁵³. Regarding the mechanisms involved in L-EV biogenesis upon B[a]P exposure, they yet
479 remain to be determined. However, it seems that neither early calcium signal triggered by PAHs,
480 neither AhR would be involved in their production.

481 Regarding the effects, notably carcinogenic, of PAHs on human health, the monitoring of the
482 populations likely exposed to these pollutants is currently performed through the measurement of
483 urinary PAH metabolites (i.e. 1-hydroxy pyrene, 3-hydroxy B[a]P), or by evaluation of DNA-adducts
484 in blood cells⁵⁴. The use of these biomarkers is difficult since their presence does not necessarily
485 reflect the level of PAH mixture humans are exposed to⁵⁴. Moreover, these biomarkers are related
486 to the capacity of cells to metabolize PAHs but not to the cellular reaction towards these pollutants.
487 Considering these aspects, it therefore seems that studying EVs in body fluids as urine would be a
488 good alternative. Indeed, EV production can be correlated to cellular response, to disease, to drug
489 exposure¹⁸. Our present results indicate that B[a]P, B[a]A and DBA are each able to up-regulate
490 production of EVs from endothelial cells. This induction effect was also observed *in vivo* upon
491 exposure to a mixture of PAHs. Thus, our data show that rat exposure (90 days) to the mixture of
492 16 US-EPA PAHs, was capable of increasing the EV disposal from urine without influencing renal

493 activity. These results therefore suggest that EVs in urine may have particular utility for monitoring
494 exposure to toxicants and to detect the related early cellular response prior to end-organ damages.

495

496 **5. Conclusion**

497 Taken together, our data indicates that, i) PAH exposure increases *in vitro* the EV production by
498 endothelial cells and *in vivo* the release of EVs in urine, and that the stimulating effects of PAHs
499 concern both S-EVs (or exosomes) and L-EVs (or microvesicles); ii) PAH exposure and more
500 particularly, exposure to B[a]P, might influence the composition of the S-EVs produced by
501 endothelial cells; and finally, iii) AhR would be involved in the PAH effects on the release of S-EVs,
502 but not L-EVs. The inability of AhR weak ligands, like PYR or B[e]P, to increase the EV production in
503 HMEC-1 cells, along with the inhibitory effects of α -NF, an AhR antagonist, towards the B[a]P effect
504 on the S-EV production strongly support this assumption. In total, our results therefore point to EVs
505 as possibly useful biomarkers of exposure for PAHs.

506

507 **References**

- 508 1. Remoundou, K. & Koundouri, P. Environmental Effects on Public Health: An Economic
509 Perspective. *Int. J. Environ. Res. Public. Health* **6**, 2160–2178 (2009).
- 510 2. Ferronato, N. & Torretta, V. Waste Mismanagement in Developing Countries: A Review of
511 Global Issues. *Int. J. Environ. Res. Public. Health* **16**, 1060 (2019).
- 512 3. Bansal, V. & Kim, K.-H. Review of PAH contamination in food products and their health
513 hazards. *Environ. Int.* **84**, 26–38 (2015).
- 514 4. Haarmann-Stemmann, T., Bothe, H. & Abel, J. Growth factors, cytokines and their receptors as
515 downstream targets of arylhydrocarbon receptor (AhR) signaling pathways. *Biochem.*
516 *Pharmacol.* **77**, 508–520 (2009).

- 517 5. Larigot, L., Juricek, L., Dairou, J. & Coumoul, X. AhR signaling pathways and regulatory
518 functions. *Biochim. Open* **7**, 1–9 (2018).
- 519 6. Bruzzoniti, M. C., Fungi, M. & Sarzanini, C. Determination of EPA's priority pollutant
520 polycyclic aromatic hydrocarbons in drinking waters by solid phase extraction-HPLC. *Anal.*
521 *Methods* **2**, 739 (2010).
- 522 7. Benedikter, B. J., Wouters, E. F. M., Savelkoul, P. H. M., Rohde, G. G. U. & Stassen, F. R. M.
523 Extracellular vesicles released in response to respiratory exposures: implications for chronic
524 disease. *J. Toxicol. Environ. Health Part B* **21**, 142–160 (2018).
- 525 8. Conde-Vancells, J., Gonzalez, E., Lu, S. C., Mato, J. M. & Falcon-Perez, J. M. Overview of
526 extracellular microvesicles in drug metabolism. *Expert Opin. Drug Metab. Toxicol.* **6**, 543–554
527 (2010).
- 528 9. Rak, J. Extracellular Vesicles – Biomarkers and Effectors of the Cellular Interactome in Cancer.
529 *Front. Pharmacol.* **4**, (2013).
- 530 10. Soekmadji, C. & Nelson, C. C. The Emerging Role of Extracellular Vesicle-Mediated Drug
531 Resistance in Cancers: Implications in Advanced Prostate Cancer. *BioMed Res. Int.* **2015**, 1–13
532 (2015).
- 533 11. Wang, J. W. *et al.* Plasma extracellular vesicle protein content for diagnosis and prognosis of
534 global cardiovascular disease. *Neth. Heart J.* **21**, 467–471 (2013).
- 535 12. Bebelman, M. P., Smit, M. J., Pegtel, D. M. & Baglio, S. R. Biogenesis and function of
536 extracellular vesicles in cancer. *Pharmacol. Ther.* **188**, 1–11 (2018).
- 537 13. Maas, S. L. N., Breakefield, X. O. & Weaver, A. M. Extracellular Vesicles: Unique
538 Intercellular Delivery Vehicles. *Trends Cell Biol.* **27**, 172–188 (2017).
- 539 14. Hartjes, T., Mytnyk, S., Jenster, G., van Steijn, V. & van Royen, M. Extracellular Vesicle
540 Quantification and Characterization: Common Methods and Emerging Approaches.
541 *Bioengineering* **6**, 7 (2019).

- 542 15. Bayraktar, R., Van Roosbroeck, K. & Calin, G. A. Cell-to-cell communication: microRNAs as
543 hormones. *Mol. Oncol.* **11**, 1673–1686 (2017).
- 544 16. Jaiswal, R. & Sedger, L. M. Intercellular Vesicular Transfer by Exosomes, Microparticles and
545 Oncosomes - Implications for Cancer Biology and Treatments. *Front. Oncol.* **9**, (2019).
- 546 17. Curtis, A. M. *et al.* Endothelial microparticles: Sophisticated vesicles modulating vascular
547 function. *Vasc. Med.* **18**, 204–214 (2013).
- 548 18. Martínez, M. C. & Andriantsitohaina, R. Extracellular Vesicles in Metabolic Syndrome. *Circ.*
549 *Res.* **120**, 1674–1686 (2017).
- 550 19. Bala, S. *et al.* Circulating microRNAs in exosomes indicate hepatocyte injury and inflammation
551 in alcoholic, drug-induced, and inflammatory liver diseases. *Hepatology* **56**, 1946–1957 (2012).
- 552 20. Benedikter, B. J. *et al.* Cigarette smoke extract induced exosome release is mediated by
553 depletion of exofacial thiols and can be inhibited by thiol-antioxidants. *Free Radic. Biol. Med.*
554 **108**, 334–344 (2017).
- 555 21. Cesselli, D. *et al.* Extracellular Vesicles: How Drug and Pathology Interfere With Their
556 Biogenesis and Function. *Front. Physiol.* **9**, (2018).
- 557 22. Palomo, L. *et al.* Abundance of Cytochromes in Hepatic Extracellular Vesicles Is Altered by
558 Drugs Related With Drug-Induced Liver Injury. *Hepatology Commun.* **2**, 1064–1079 (2018).
- 559 23. Pollet, H., Conrard, L., Cloos, A.-S. & Tyteca, D. Plasma Membrane Lipid Domains as
560 Platforms for Vesicle Biogenesis and Shedding? *Biomolecules* **8**, 94 (2018).
- 561 24. Turturici, G., Tinnirello, R., Sconzo, G. & Geraci, F. Extracellular membrane vesicles as a
562 mechanism of cell-to-cell communication: advantages and disadvantages. *Am. J. Physiol.-Cell*
563 *Physiol.* **306**, C621–C633 (2014).
- 564 25. Mayati, A. *et al.* Induction of Intracellular Calcium Concentration by Environmental Benzo(*a*
565)pyrene Involves a β 2-Adrenergic Receptor/Adenylyl Cyclase/Epac-1/Inositol 1,4,5-
566 Trisphosphate Pathway in Endothelial Cells. *J. Biol. Chem.* **287**, 4041–4052 (2012).

- 567 26. Tekpli, X. *et al.* Membrane remodeling, an early event in benzo[α]pyrene-induced apoptosis.
568 *Toxicol. Appl. Pharmacol.* **243**, 68–76 (2010).
- 569 27. Pergoli, L. *et al.* Extracellular vesicle-packaged miRNA release after short-term exposure to
570 particulate matter is associated with increased coagulation. *Part. Fibre Toxicol.* **14**, (2017).
- 571 28. Ryu, A.-R., Kim, D. H., Kim, E. & Lee, M. Y. The Potential Roles of Extracellular Vesicles in
572 Cigarette Smoke-Associated Diseases. *Oxid. Med. Cell. Longev.* **2018**, 1–8 (2018).
- 573 29. Kranendonk, M. E. *et al.* Extracellular vesicle markers in relation to obesity and metabolic
574 complications in patients with manifest cardiovascular disease. *Cardiovasc. Diabetol.* **13**, 37
575 (2014).
- 576 30. Iba, T. & Ogura, H. Role of extracellular vesicles in the development of sepsis-induced
577 coagulopathy. *J. Intensive Care* **6**, (2018).
- 578 31. Barreiro, K. & Holthofer, H. Urinary extracellular vesicles. A promising shortcut to novel
579 biomarker discoveries. *Cell Tissue Res.* **369**, 217–227 (2017).
- 580 32. Lv, L.-L., Feng, Y., Tang, T.-T. & Liu, B.-C. New insight into the role of extracellular vesicles
581 in kidney disease. *J. Cell. Mol. Med.* **23**, 731–739 (2019).
- 582 33. Pisitkun, T., Shen, R.-F. & Knepper, M. A. Identification and proteomic profiling of exosomes
583 in human urine. *Proc. Natl. Acad. Sci.* **101**, 13368–13373 (2004).
- 584 34. Grova, N., Faÿs, F., Hardy, E. M. & Appenzeller, B. M. R. New insights into urine-based
585 assessment of polycyclic aromatic hydrocarbon-exposure from a rat model: Identification of
586 relevant metabolites and influence of elimination kinetics. *Environ. Pollut.* **228**, 484–495
587 (2017).
- 588 35. Fernández-Llama, P. *et al.* Tamm-Horsfall protein and urinary exosome isolation. *Kidney Int.*
589 **77**, 736–742 (2010).
- 590 36. Musante, L. *et al.* A Simplified Method to Recover Urinary Vesicles for Clinical Applications
591 and Sample Banking. *Sci. Rep.* **4**, 7532 (2015).

- 592 37. Théry, C., Amigorena, S., Raposo, G. & Clayton, A. Isolation and Characterization of
593 Exosomes from Cell Culture Supernatants and Biological Fluids. *Curr. Protoc. Cell Biol.* **30**,
594 3.22.1-3.22.29 (2006).
- 595 38. Brinchmann, B. *et al.* Lipophilic Chemicals from Diesel Exhaust Particles Trigger Calcium
596 Response in Human Endothelial Cells via Aryl Hydrocarbon Receptor Non-Genomic
597 Signalling. *Int. J. Mol. Sci.* **19**, 1429 (2018).
- 598 39. Brinchmann, B. C. *et al.* Lipophilic components of diesel exhaust particles induce pro-
599 inflammatory responses in human endothelial cells through AhR dependent pathway(s). *Part.*
600 *Fibre Toxicol.* **15**, 21 (2018).
- 601 40. Head, B. P., Patel, H. H. & Insel, P. A. Interaction of membrane/lipid rafts with the
602 cytoskeleton: Impact on signaling and function. *Biochim. Biophys. Acta BBA - Biomembr.* **1838**,
603 532–545 (2014).
- 604 41. Record, M., Silvente-Poirot, S., Poirot, M. & Wakelam, M. J. O. Extracellular vesicles: lipids as
605 key components of their biogenesis and functions. *J. Lipid Res.* **59**, 1316–1324 (2018).
- 606 42. Holme, J. A., Brinchmann, B. C., Le Ferrec, E., Lagadic-Gossman, D. & Øvrevik, J.
607 Combustion Particle-Induced Changes in Calcium Homeostasis: A Contributing Factor to
608 Vascular Disease? *Cardiovasc. Toxicol.* **19**, 198–209 (2019).
- 609 43. Tekpli, X., Holme, J. A., Sergent, O. & Lagadic-Gossman, D. Role for membrane remodeling
610 in cell death: Implication for health and disease. *Toxicology* **304**, 141–157 (2013).
- 611 44. Yáñez-Mó, M. *et al.* Biological properties of extracellular vesicles and their physiological
612 functions. *J. Extracell. Vesicles* **4**, 27066 (2015).
- 613 45. van Meteren, N. *et al.* Polycyclic aromatic hydrocarbons can trigger a hepatocyte release of
614 extracellular vesicles by various mechanisms of action depending on their affinity for aryl
615 hydrocarbon receptor. *Toxicol. Sci.* (2019). doi:10.1093/toxsci/kfz157

- 616 46. Hardonnière, K., Huc, L., Sergent, O., Holme, J. A. & Lagadic-Gossmann, D. Environmental
617 carcinogenesis and pH homeostasis: Not only a matter of dysregulated metabolism. *Semin.*
618 *Cancer Biol.* **43**, 49–65 (2017).
- 619 47. Nawaz, M., Fatima, F. & Squire, J. A. Mining Extracellular Vesicles for Clinically Relevant
620 Noninvasive Diagnostic Biomarkers in Cancer. in *Novel Implications of Exosomes in Diagnosis*
621 *and Treatment of Cancer and Infectious Diseases* (ed. Wang, J.) (InTech, 2017).
622 doi:10.5772/intechopen.69406
- 623 48. Abels, E. R. & Breakefield, X. O. Introduction to Extracellular Vesicles: Biogenesis, RNA
624 Cargo Selection, Content, Release, and Uptake. *Cell. Mol. Neurobiol.* **36**, 301–312 (2016).
- 625 49. Reiners, J. J. & Clift, R. E. Aryl Hydrocarbon Receptor Regulation of Ceramide-induced
626 Apoptosis in Murine Hepatoma 1c1c7 Cells: a function independent of aryl hydrocarbon
627 receptor nuclear translocator. *J. Biol. Chem.* **274**, 2502–2510 (1999).
- 628 50. Wang, H.-C. *et al.* Aryl hydrocarbon receptor signaling promotes ORMDL3-dependent
629 generation of sphingosine-1-phosphate by inhibiting sphingosine-1-phosphate lyase. *Cell. Mol.*
630 *Immunol.* (2018). doi:10.1038/s41423-018-0022-2
- 631 51. Verderio, C., Gabrielli, M. & Giussani, P. Role of sphingolipids in the biogenesis and biological
632 activity of extracellular vesicles. *J. Lipid Res.* **59**, 1325–1340 (2018).
- 633 52. Jorfi, S. & Inal, J. M. The role of microvesicles in cancer progression and drug resistance.
634 *Biochem. Soc. Trans.* **41**, 293–298 (2013).
- 635 53. Shedden, K., Xie, X. T., Chandaroy, P., Chang, Y. T. & Rosania, G. R. Expulsion of Small
636 Molecules in Vesicles Shed by Cancer Cells: Association with Gene Expression and
637 Chemosensitivity Profiles^{1,2}. *Cancer Res* **63**, 4331–7 (2003).
- 638 54. Srogi, K. Monitoring of environmental exposure to polycyclic aromatic hydrocarbons: a review.
639 *Environ. Chem. Lett.* **5**, 169–195 (2007).

640

641

642 **Acknowledgements**

643 We first wish to thank Dr Carmen Martinez (UMR Inserm 1063, Angers, France) for valuable
644 discussion on EVs at the beginning of this project. We are also very grateful to the MRiC platform
645 (UMS BIOSIT, Rennes, France), notably Stéphanie Dutertre for training us on calcium measurements.
646 This study was financially supported by the “Programme Environnement-Santé-Travail” of Anses
647 with the funding from ITMO cancer in the context of the Cancer Plan 2014-2019 (EST-2016/1/31),
648 and by the Cancéropôle Grand-Ouest/Région Bretagne (Concerto project). Manon Le Goff was a
649 recipient of a PhD fellowship from the Collectivités Locales Mayennaises.

650 **Figure legends**

651 **Figure 1. B[a]P stimulates the extracellular vesicle release from endothelial HMEC-1 cells.** Total
652 EVs were isolated by ultracentrifugation and analyzed by Nanoparticle Tracking Analysis (NTA). **(A)**
653 EVs released per HMEC-1 cells exposed to vehicle (DMSO) or 1 nM to 10 000 nM B[a]P for 24 h, and
654 **(B)** exposed to 100 nM B[a]P from 2 h to 24 h. **(C)** Size distribution profile by NTA of EVs produced
655 by endothelial cells during 24h at 100 nM B[a]P. Data are the means \pm SEM of three or more
656 independent assays. *p < 0.05; **p < 0.01; ***p < 0.001 significantly different from unexposed
657 control.

658 **Figure 2. B[a]P stimulates the production of both small vesicles (S-EVs) and large (L-EVs) vesicles**
659 **from endothelial HMEC-1 cells.** HMEC-1 cells were exposed to vehicle (DMSO) or 100 nM B[a]P for
660 24 h. S-EVs and L-EVs were isolated by differential ultracentrifugation, as described in Material and
661 Methods section. Size distribution profile, determined by Nanoparticle Tracking Analysis (NTA) and
662 amount (inserts) of S-EVs **(A)** and L-EVs **(B)** released per endothelial cell. Data are the means \pm SEM
663 of three or more independent assays. *p < 0.05; **p < 0.01 significantly different from unexposed
664 control.

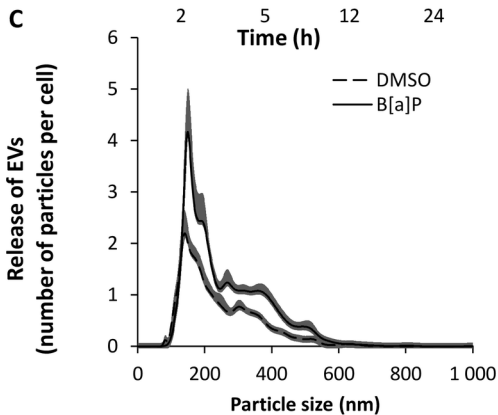
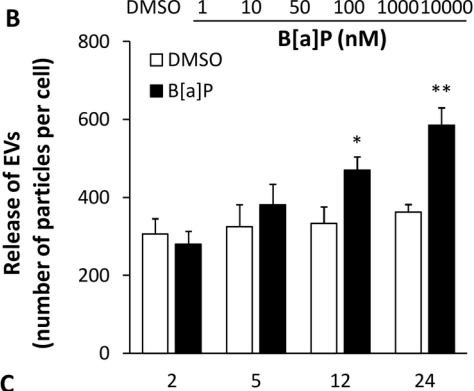
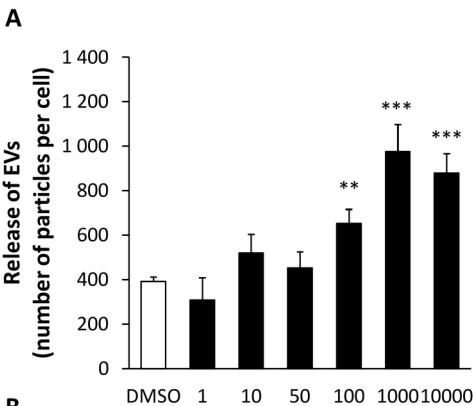
665 **Figure 3. Characterization of S-EV and L-EV populations isolated from endothelial HMEC-1 cells.**
666 HMEC-1 cells were exposed to vehicle (DMSO) or 100 nM B[a]P for 24 h. S-EVs and L-EVs were
667 isolated by differential ultracentrifugation, as described in Material and Methods section. **(A)**
668 Transmission electron microscopy pictures of S-EV and L-EV pellets (scale bars = 200 nm). **(B)**
669 Western blot analysis of EV markers in S-EVs and L-EVs obtained from HMEC-1. Cell lysates were
670 used as positive control for each marker studied. Lamin A/C was used to evaluate nuclear sample
671 contamination; caveolin-1, flotillin-1, TSG101 and β -actin were used as markers of both S-EVs and L-
672 EVs. CD63 was used as S-EV specific markers, and Hsc70 was used as loading control. **(C)**
673 Measurement of annexin V positivity of L-EVs by flow cytometry. Annexin V was used as marker for
674 phosphatidylserine. Results are expressed as a percentage of isolated L-EVs.

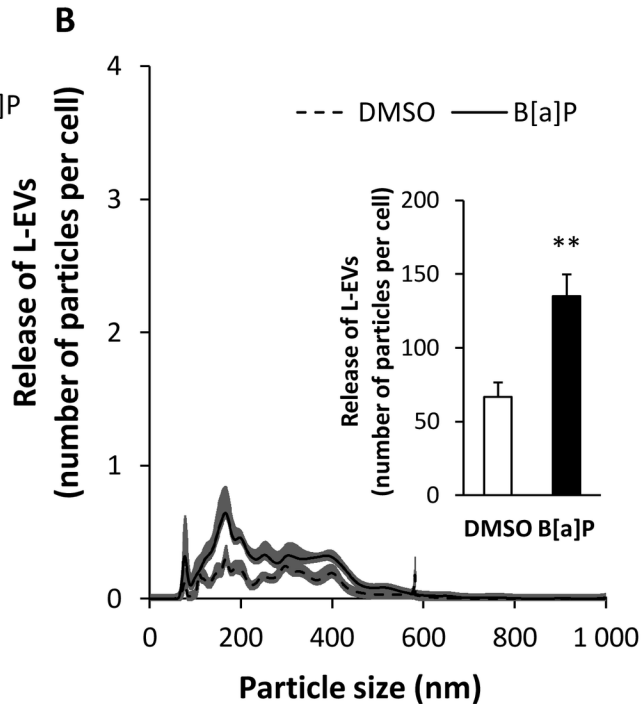
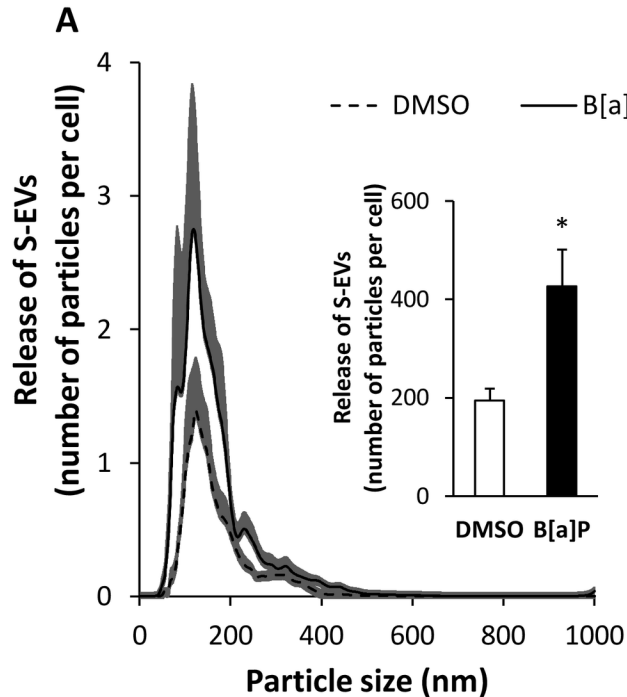
675 **Figure 4. Effects of PAHs on the EVs released from endothelial HMEC-1 cells.** (A-F) HMEC-1 cells
676 were exposed to vehicle (DMSO) or 100 nM of B[e]P, PYR, B[A]A, B[a]P or DBA for 24 h. (A) mRNA
677 expression of CYP1A1 and CYP1B1 was analyzed using RT-qPCR. Data are expressed relatively to
678 mRNA levels of CYP1A1 and CYP1B1 found in corresponding control cells (DMSO), arbitrarily set to
679 1 unit. (B-F) Total EVs were isolated by ultracentrifugation and analyzed by Nanoparticle Tracking
680 Analysis (NTA). (B) EV production released per HMEC-1 cells exposed to different PAHs for 24 h. (C-
681 F) Size distribution profile by NTA of EVs produced by endothelial cells during a 24 h exposure with
682 different PAHs compared to control (DMSO). Data are the means \pm SEM of three or more
683 independent assays. *p < 0.05; **p < 0.01; ***p < 0.001 significantly different from unexposed
684 control.

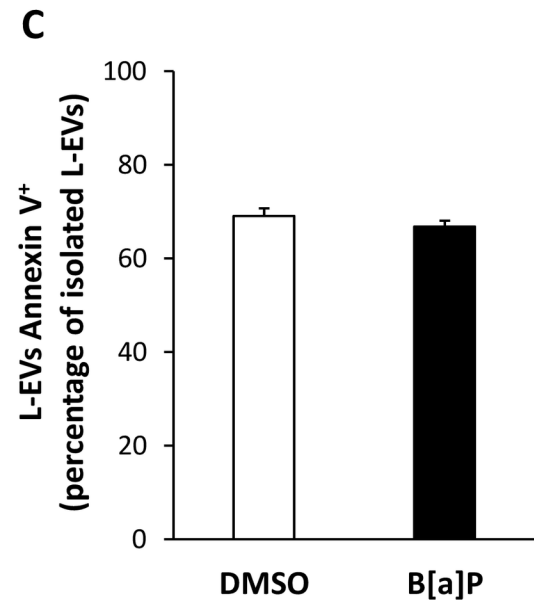
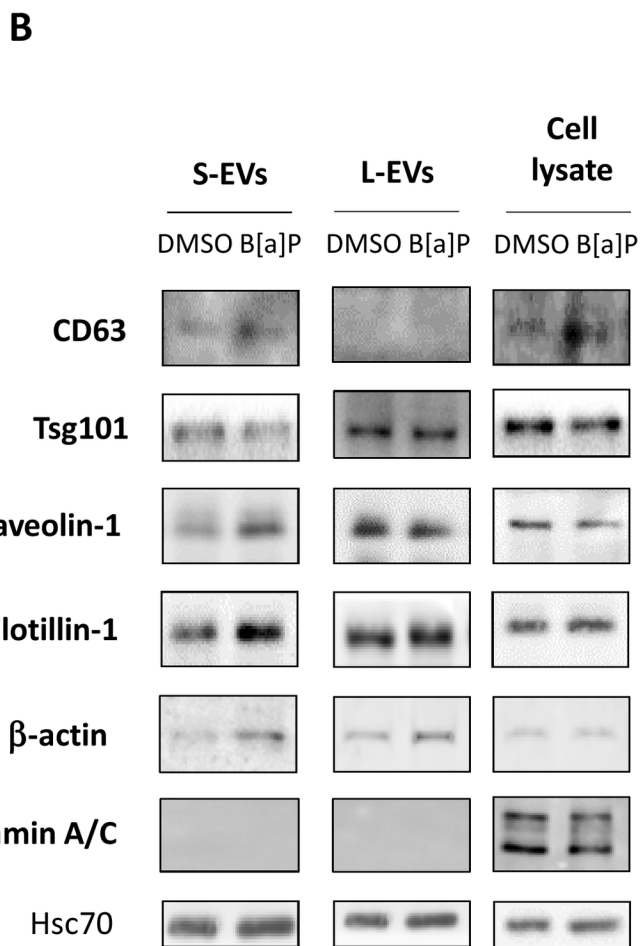
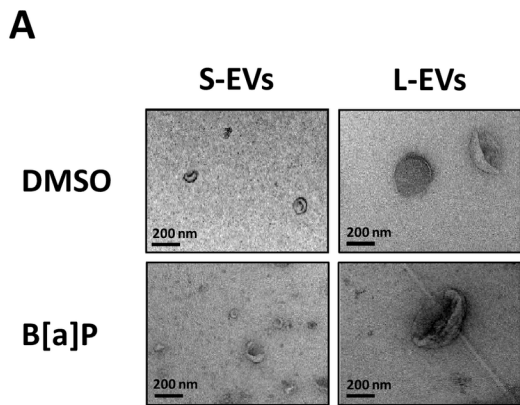
685 **Figure 5: Involvement of AhR in the production of S-EVs, but not of L-EVs, produced upon B[a]P**
686 **exposure of endothelial HMEC-1 cells.** HMEC-1 cells were exposed to vehicle (DMSO) or 100 nM
687 B[a]P in presence or not to AhR antagonist α -NF (10 μ M). S-EVs and L-EVs were isolated by
688 differential ultracentrifugation, as described in Material and Methods section. S-EV (A) and L-EV (B)
689 concentrations released per endothelial cell were determined by Nanoparticle Tracking Analysis
690 (NTA). Data are the means \pm SEM of three or more independent assays. *p < 0.05 significantly
691 different from unexposed control. #p < 0.05 significantly different from B[a]P-treated cells.

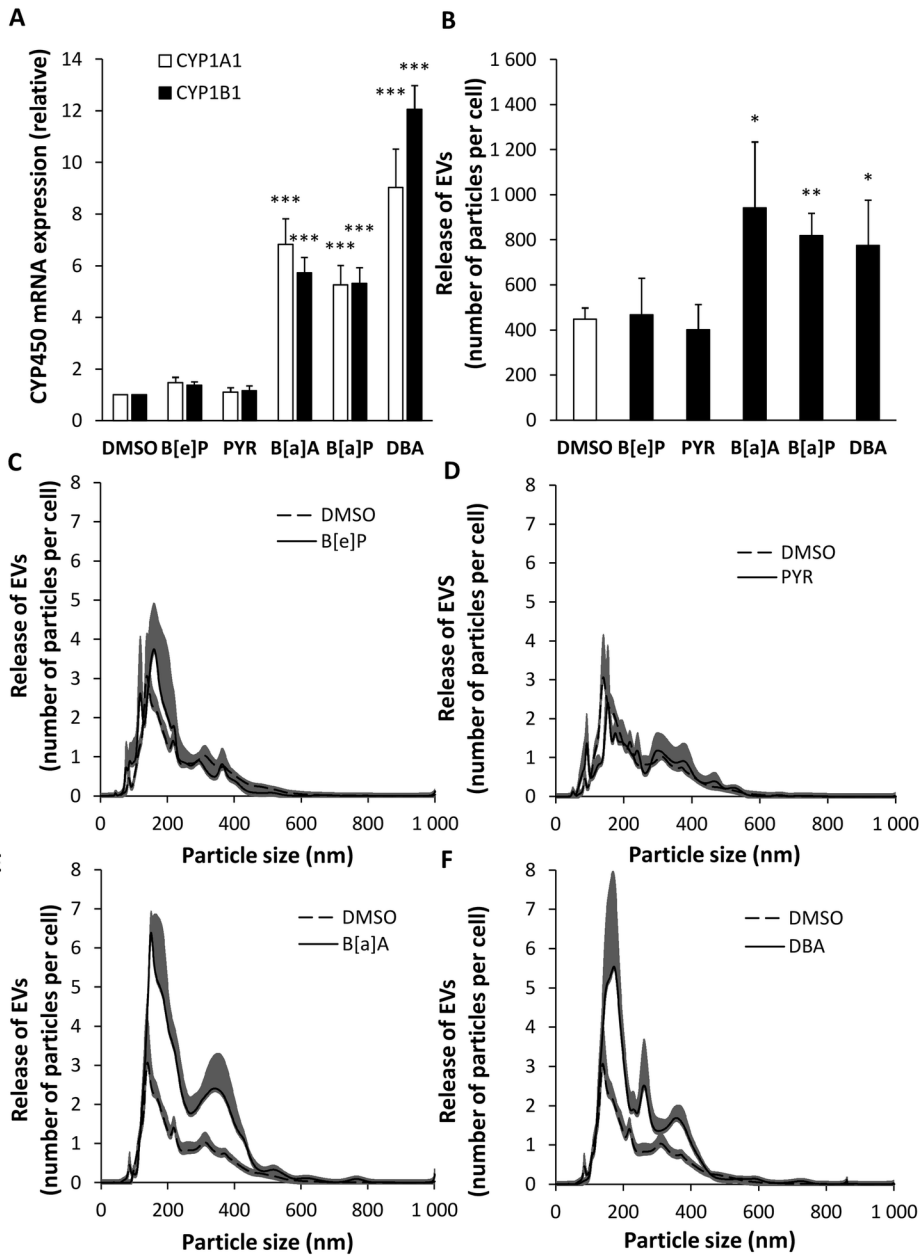
692 **Figure 6. PAH effects on intracellular Ca²⁺ concentrations ([Ca²⁺]_i) and on the apoptosis in HMEC-**
693 **1 cells.** HMEC-1 cells were exposed to vehicle (DMSO) or 100 nM of B[e]P, PYR, B[A]A, B[a]P or DBA.
694 (A) [Ca²⁺]_i in cells was analyzed by real time fluorescence imaging, using Ca²⁺-sensitive probe Fura2-
695 AM (acetoxymethyl ester). Data were expressed as normalized maximum delta ratio as described in
696 Materials and Methods. HMEC-1 cells were treated by B[e]P, PYR, B[A]A, B[a]P or DBA at 100 nM or
697 untreated (DMSO) during 24 h for the evaluation of cytotoxicity by (B) counting apoptotic cells. Data
698 are the means \pm SEM of three or more independent assays. *p < 0.05; **p < 0.01; ***p < 0.001
699 significantly different from unexposed control.

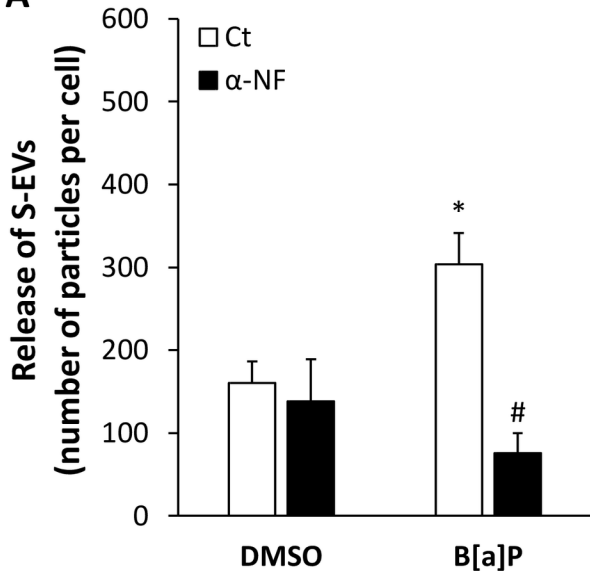
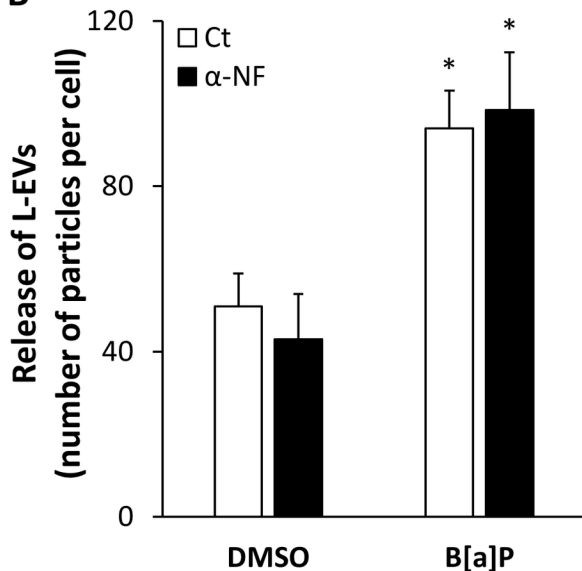
700 **Figure 7. *In vivo* PAH exposure increases EV amount in urine.** Rats received 0.8 mg/kg of a 16 PAH
701 mixture or only vehicle for control rats during 90 days. At the end of 90 days-experiment, urine
702 fractions were collected over a 24 h period. EVs were isolated by differential ultracentrifugation. **(A)**
703 EV concentrations released per mL of urine were assessed by Nanoparticle Tracking Analysis. **(B)**
704 Creatinine concentration (mg/mL) in urine of rats. **(C)** Urinary volume produced during the last 24
705 hours of PAH exposure. Data are the means \pm SEM of four rats. ***p < 0.001 significantly different
706 from unexposed control.

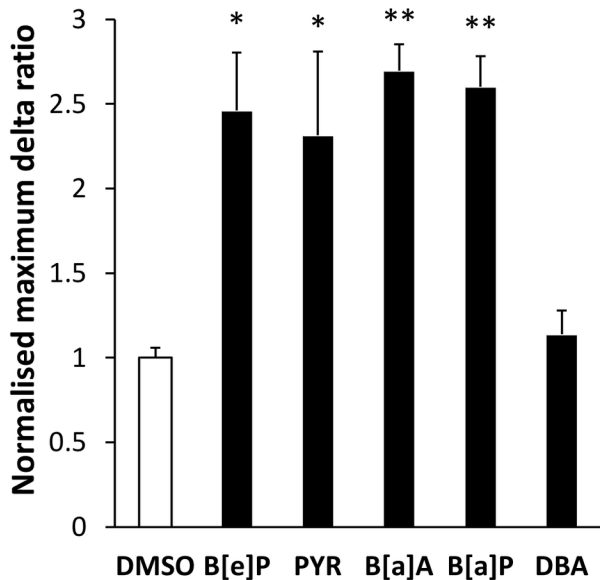








A**B**

A**B**